Biogeosciences
Discussions

Open Access

Distribution of Arctic and Pacific copepods and their habitat in the northern Bering Sea and Chukchi Sea

H. Sasaki[1,2], K. Matsuno[1,2], A. Fujiwara[3], M. Onuka[4], A. Yamaguchi[2], H. Ueno[2], Y. Watanuki[2], and T. Kikuchi[3]

[1]Arctic Environment Research Center, National Institute of Polar Research, 10-3 Midori-cho, Tachikawa, Tokyo 190-8518, Japan
[2]Graduate School of Fisheries Sciences, Hokkaido University, 3-1-1 Minato-cho, Hakodate, Hokkaido 041-8611, Japan
[3]Japan Agency for Marine-Earth Science and Technology, 2-15 Natsushima-cho, Yokosuka, Kanagawa 237-0061, Japan
[4]Graduate School of Environmental Science, Hokkaido University, N10W5, Sapporo, Hokkaido 060-0810, Japan

Correspondence to: H. Sasaki (hiro_sasaki@salmon.fish.hokudai.ac.jp)

BGD

12, 18661–18691, 2015

Distribution of Arctic and Pacific copepods and their habitat

H. Sasaki et al.

Title Page

Abstract	Introduction
Conclusions	References
Tables	Figures

|◄ ►|

◄ ►

Back Close

Full Screen / Esc

Printer-friendly Version

Interactive Discussion

Abstract

The advection of warm Pacific water and the reduction of sea-ice extent in the western Arctic Ocean may influence the abundance and distribution of copepods, i.e., a key component in food webs. To understand the factors affecting abundance of copepods in the northern Bering Sea and Chukchi Sea, we constructed habitat models explaining the spatial patterns of the large and small Arctic copepods and the Pacific copepods, separately, using generalized additive models. Copepods were sampled by NORPAC net. Vertical profiles of density, temperature and salinity in the seawater were measured using CTD, and concentration of chlorophyll *a* in seawater was measured with a fluorometer. The timing of sea-ice retreat was determined using the satellite image. To quantify the structure of water masses, the magnitude of pycnocline and averaged density, temperature and salinity in upper and bottom layers were scored along three axes using principal component analysis (PCA). The structures of water masses indexed by the scores of PCAs were selected as explanatory variables in the best models. Large Arctic copepods were abundant in the water mass with high salinity water in bottom layer or with cold/low salinity water in upper layer and cold/high salinity water in bottom layer, and small Arctic copepods were abundant in the water mass with warm/saline water in upper layer and cold/high salinity water in bottom layers, while Pacific copepods were abundant in the water mass with warm/saline in upper layer and cold/high salinity water in bottom layer. All copepod groups were abundant in areas with deeper depth. Although chlorophyll *a* in upper and bottom layers were selected as explanatory variables in the best models, apparent trends were not observed. All copepod groups were abundant where the sea-ice retreated at earlier timing. Our study might indicate potential positive effects of the reduction of sea-ice extent on the distribution of all groups of copepods in the Arctic Ocean.

1 Introduction

The Arctic sea-ice reduction is remarkable during these decades and has been a public concern as this may cause the changes in marine ecosystem in Arctic Ocean. Arctic marine food webs are supported by primary production in the seasonal sea-ice zone and profoundly influenced by the timing of blooming of the ice algae and the timing of stabilization of water column by formation of sea-ice (Grebmeier, 2012). The recent sea-ice reduction progresses the timing of phytoplankton bloom (Hunt et al., 2002, 2011; Kahru et al., 2011) and increases the annual primary production (Arrigo et al., 2008). However, Clement et al. (2004) suggested that the earlier sea-ice retreat leads the stratification, the trapping of the nutrient in the surface and lower primary production with insufficient sunlight. In Arctic, food webs are short and efficient, even small changes in production pathways can affect on higher trophic organisms (Grebmeier et al., 2006). The change of the timing and location of primary production and associated grazing by zooplankton have a direct influence on the energy and material transfer to benthic community (Grebmeier et al., 2010). Thus recent reduction of sea-ice extent leads shifts in the distribution of benthos, fishes and marine mammals (Mueter and Litzow, 2008; Doney et al., 2012). Further these shifts in the species distributions may change the interaction of species including predation and competition (Moore and Huntington, 2008).

The northern Bering Sea and Chukchi Sea may be amongst regions where the seasonal sea-ice coverage has been changed drastically in this decade (Comiso et al., 2008; Parkinson and Comiso, 2013), possibly because of the increase of the inflow of the Pacific water from the Bering Sea through the Bering Strait (Shimada et al., 2006). In these seas, the water masses have been identified based on salinity and temperature (Table 1). Water masses include warmer/low salinity Alaskan coastal water (ACW; temperature 2.0–13.0 and salinity < 31.8 °C) originated from the eastern Bering Sea; warm/saline Bering shelf water (BSW; 0.0–10.0 and 31.8–33.0 °C) originated on the middle Bering shelf; cold/higher salinity Anadyr Water (AW; −1.0–1.5 and

32.3–33.3 °C) originated from the Gulf of Anadyr at the depth along the continental shelf of the Bering Sea; BSW and AW merged into Bering Sea Anadyr water (BSAW) (Coachman et al., 1975; Springer et al., 1989). Further, cold/lower salinity ice melt water (IMW; < 2.0 and < 30.0 °C) originates from sea-ice and colder/high salinity dense water (DW; < -1.0 and 32.0–33.0 °C) formed in the previous winter during freezing over the both Bering Sea and Chukchi Sea (Weingartner et al., 2013) are identified. These water masses often show vertical settings geographically and seasonally (Iken et al., 2010; Eisner et al., 2013; Weingartner et al., 2013).

In the northern Bering Sea and Chukchi Sea, copepods are primary consumers of phytoplankton and are main prey of forage fish (e.g., Polar cod *Boreogadus saida*, Nakano et al., 2015), seabirds (e.g., Phalaropes, Shearwaters and Crested Auklets *Aethia cristatella*, Piatt and Springer, 2003; Hunt et al., 2013), and baleen whales (e.g., Bowhead whale *Balaena mysticetus*, Lowry et al., 2004). Therefore, copepods could be a key component in the Arctic marine food webs (Lowry et al., 2004). The communities of copepods are associated with the structure of water masses (e.g., Springer et al., 1989; Hopcroft et al., 2010; Eisner et al., 2013); *Pseudocalanus* species are abundant in the ACW and Pacific species are abundant in the AW. To quantify the response of copepods to the recent reduction of sea-ice extent, environmental factors affecting their distributions have to be explored more systematically and quantitatively. In this region, large sized Arctic copepods (*Calanus glacialis*) and small sized Arctic copepod (e.g., *Acartia hudsonica*, *Centropages abdominalis*, *Eurytemora herdmani* and *Pseudocalanus acuspes*) are distributed (Springer et al., 1996). Also Pacific copepods (*Calanus marshallae*, *Eucalanus bungii*, *Meridia pacifica*, *Neocalunus cristatus*, *N. flemingeri* and *N. plumchrus*) are often transported from the Bering Sea (Lane et al., 2008; Hopcroft et al., 2010). Therefore, for communities of copepods in this region, the inflow of warm Pacific water as well as the reduction of sea-ice extent may be important factor. In 2007, for an example, sea-ice disappeared at earliest and its coverage was minimum and water temperature was highest and annual transport of the Pacific water was greatest during these 17 years (Woodgate et al., 2010, 2012). Then Pacific cope-

pod species (e.g., *Eucalanus bungii*) expanded its distribution into the Chukchi Sea in 2007 (Matsuno et al., 2011). To predict these responses of zooplankton to the environmental changes can be happened in future, it is important to understand the tendency of the spatial patterns of the abundance of zooplankton and the key environmental factors for them by using statistical model, quantitatively.

The objective of this study is to examine the factors affecting the spatial pattern of the abundance of copepods based on the data collected by T/S *Oshoro-maru* in the summer of 2007, 2008 and 2013. We categorized copepods into three groups; large and small Arctic, and Pacific copepod. Life cycles of large Arctic copepods are one or less generation per year, while that of small Arctic copepods are multiple generations in Arctic (e.g., Dvoretsky and Dvoretsky, 2009; Falk-Peterson et al., 2009). Pacific copepods are only advected from the Pacific Ocean through the Bering Strait and not established in Arctic Ocean (Springer et al., 1989; Matsuno et al., 2015). To quantify the factors affecting the spatial pattern of abundance of each copepods group, we used the Generalized Additive Models (GAMs). The relationships between the abundance of copepods and traditionally defined water masses are reported (Hopcroft and Kosobokova, 2010; Eisner et al., 2013) where the surface and bottom water masses were characterized based on the temperature and salinity. However, it is difficult to evaluate the effects of complicated water properties quantitatively on the abundance of copepods. To apply GAMs, explanatory variables that were correlated with other variable have to be removed to avoid the problem of multi co-linearity. This procedure may fail to denote the important oceanographic features such as the combination of water masses in upper and bottom layers since temperature and salinity of waters in both layers are often correlated strongly. In this study, to denote the combination of water masses in upper and bottom, we summarized the water mass properties in upper and bottom layers into the scores using principal component analyses (PCA). These scores can be used as continuous explanatory variables in the habitat models.

Distribution of Arctic
and Pacific copepods
and their habitat

H. Sasaki et al.

2 Materials and Methods

2.1 Field sampling

The survey was conducted by T/S *Oshoro-maru* (1392 t) Hokkaido University during 30 July–24 August 2007 (31 stations), 30 June–13 July 2008 (26 stations) and 4–17 July 2013 (31 stations) (Fig. 1). Zooplankton samples were collected at day or night by vertical tows with a NORPAC net (mouth diameter 45 cm, mesh size 335 µm) from 5 m above the bottom to the surface (depths of most stations were about 50 m). The volume of water filtered through the net was estimated using a flow-meter mounted in the mouth of the net. Zooplankton samples were immediately preserved with 5 % *v*/*v* borax buffered formalin. In the land laboratory, identification and enumeration with taxa were performed on the zooplankton samples under a stereomicroscope. For dominant taxa (calanoid copepods), identification was made with species. Depended on distribution, generation length and reproduction of copepods referred Falk-Petersen et al. (2009) and Dvoretsky and Dvoretsky (2009), and we summarized the copepods species into three groups: large Arctic (Cop_{arc}-L, generation length is more than one year and reproduction occur at one time), small Arctic (Cop_{arc}-S, generation length is less than one year and multi-times reproduction occur in a year) and Pacific copepods (Cop_{pac}, generation length is more than one year and reproduction occur at one time) (Table 2). At zooplankton sampling station, vertical profile of temperature and salinity were measured by Conductivity Temperature Depth (CTD: Sea-Bird Electronics Inc., SBE 911 Plus) casts. Chlorophyll *a* was sampled by the water samples with Niskin bottles on the CTD rosette from the bottom (21–56 m) to surface. Water samples were filtered at low pressure onto GF/F filters. Then, phytoplankton pigments on filters were extracted by *N*, *N*-dimethylformamide (Suzuki and Ishimaru, 1990), and chlorophyll *a* concentrations were determined by fluorometric method using a Turner Designs 10-AU fluorometer (Welschmeyer, 1994). In order to investigate the relationships between the abundance of copepods and sea-ice condition, we derived SSM/I Daily Polar Gridded

Sea Ice Concentration (SIC) data, calculated by using NASA Team, from the National Snow and Ice Data Center (http://nsidc.org/).

2.2 Data analysis

We divided the water column into two layers; i.e., the layers above and under the pycnocline and defined them as the upper and bottom layers, respectively. The pycnocline was defined as the depth of maximum density gradient. The density (ρ) was calculated from temperature and salinity measured by CTD profiles with a vertical data resolution of 1 m. Then, we calculated vertical density gradient ($\frac{d\rho}{dD}$) at each depth (D). We defined the depth of the maximum $\frac{d\rho}{dD}$ (hereafter $\frac{d\rho}{dD}_{max}$) as the depth of maximum density gradient ($D_{\frac{d\rho}{dD}_{max}}$). In this approach, to examine the water mass properties at the upper and bottom layers, environments (temperature, salinity and log-transformed chlorophyll a) were vertically averaged within the upper and bottom layers (i.e., above and under $D_{\frac{d\rho}{dD}_{max}}$) and defined them as T_{UPP}, T_{BOT}, S_{UPP}, S_{BOT}, Chl a_{UPP} and Chl a_{BOT}, respectively (see Table 3). Principal component analysis (PCA) was applied to determine water mass structure using $\frac{d\rho}{dD}_{max}$, T_{UPP}, T_{BOT}, S_{UPP} and S_{BOT} at all 88 stations together. Because principal water masses in the Bering Sea and Chukchi Sea were characterized by temperature and salinity of water column (Coachman et al., 1975), Chl.a_{UPP}, Chl.a_{BOT} and SIC were not used in PCA for determining structure of water masses. Given these five parameters in PCA were standardized prior to analysis to reduce problems with unequal variation and expected nonlinearity. Several principal components and its factor loadings (correlations of factors to the derived principal components) are presented. The scores of PCAs were used as covariates of water mass structures in the habitat models. In addition, we used the anomaly of timing of sea-ice retreat (aTSR) at each sampling station as index of sea-ice condition. aTSR was calculated using satellite derived sea-ice image in 1991–2013. Although sea-ice concentration images had been projected to polar stereographic coordinates with a 25 km spatial resolution, we interpolated them using the nearest neighbour method and resampled

|◄ | ►|

◄ | ►

Back | Close

Full Screen / Esc

Printer-friendly Version

Interactive Discussion

them into 9 km spatial resolution. Considering the missing value and land contamina-tions, we defined SIC $< 50\%$ as non-ice covered pixels, and aTSR was defined as the anomalous last date when the SIC fell below 50% prior to the date of annual sea-ice minimum in the Arctic Ocean.

2.3 Statistical analysis

Prior to conducting the habitat models, we examined the multi co-linearity between the explanatory variables by correlation analysis. To examine the relationships between copepods abundance (large and small Arctic, and Pacific copepods) and environments, we constructed the habitat models using Generalized Additive Models (GAMs). GAMs are a non-parametric extension of Generalized Linear Models (GLMs) such as multiple regression models (Eq. 1); with the only underlying assumption that functions are ad-ditive and that the components are smooth (Eq. 2). The basic concept is replacement of the parametric GLMs structure:

$$g(\mu) = \alpha + \beta_1 x_1 + \beta_2 x_2 + \beta_3 x_3 + \cdots + \beta_i x_i \tag{1}$$

with the additive smoothing function structure:

$$g(\mu) = \varepsilon + s_1(x_1) + s_2(x_2) + s_3(x_3) + \cdots + s_i(x_i) \tag{2}$$

where the α and the ε are the intercepts, and the β_i and the s_i are coefficients and smooth functions of covariates, respectively. To select the most adequate model in our approach, we used Akaike's Information Criteria. Then model validation was applied on the optimal models to verifying assumptions and reproducibility. Specifically, we plotted original value vs. fitted value, and judged the adequacy of our optimal models based on R^2. Deviance explained indicated how many percent can explain the variance of the most adequate model. All statistical analyses were undertaken using R (version.2.15.0 http://www.r-project.org).

3 Results

3.1 Principal component analysis and water mass

The first principal component explained 47.1 % of total variability. In the score of first principal component (PC1), the coefficient of loading was positive for $\frac{d\rho}{dD}_{max}$, indicating that the magnitude of stratification increased with increasing PC1, while strongly negative for T_{UPP} and T_{BOT}, indicating that the temperature in the whole of water mass was lower with higher PC1 (Table 4). And also, it was negative for S_{UPP} indicating that there was low salinity water mass in the surface layer with higher PC1, while weakly positive for S_{BOT}. According to Fig. 2a showing the $T–S$ diagram coloured by the score of PC1, the higher PC1 (> 1) value indicated the combination of the cold/lower salinity ice-melt water (IMW) in upper layer and the colder/high salinity dense water (DW) in bottom layer. On the contrary, low PC1 indicated the warm water mass in both layers and/or low salinity water in the surface (Table 4). According to Fig. 2a, lower PC1 (< -1.5) value indicated the combination with warmer/low salinity Alaskan coastal water (ACW) in the upper layer and warm/saline Bering shelf water (BSW) or cold/higher salinity Anadyr Water (AW) or merged water (BSAW) in bottom layer. When the score of PC1 showed low–medium (-1.5–0.5), it indicated the combination of water mass with BSW and AW or BSAW (Fig. 2a). PC1 was higher at the stations north of 69° N than the southern ones in 2008 and 2013 and low for all stations in 2007 (Fig. 3), indicating that the combination of IMW and DW was dominant in the northern stations in 2008 and 2013, and ACW was dominant at almost all stations in 2007.

The second principal component explained 34.8 % of total variability. In the score of second principal component (PC2), the coefficient of loading was negative for $\frac{d\rho}{dD}_{max}$ and temperature, and positive for salinity at both upper and bottom layers (Table 4). These indicated that there was the highly saline water at both layers which leads to decrease the magnitude of stratification and become single layered structure with higher PC2. Shown in Fig. 2b, the medium–high PC2 (> 0.5), indicated waters with single-layered structure, warm/saline BSW or colder/higher salinity AW or BSAW, and the

low–medium PC2 (< 0.5), indicated water with two-layered structure, warmer temperature and lower saline waters at upper layer comparing bottom layers–IMW at upper layer and DW at bottom layer, or ACW at upper layer and BSW or AW or BSAW at bottom layer. PC2 tended to be high at the station $< 69°$ N in all years and low at the station east of the survey area in 2007 (Fig. 4), indicating that single layered structure with BSW or AW or BSAW was dominant in the Bering Strait, however, the combination with ACW, and BSW or AW or BSAW in the northeast of survey area in 2007.

The third principal component explained 14.2 % of total variability. The score of third principal component (PC3) correlated positively with all physical variables (Table 4), especially positive correlated especially with T_{UPP} and S_{BOT}. According to $T-S$ diagram, coloured by the value of PC3 (Fig. 2c), relatively high PC3 (> 0.5) with warmer T_{UPP} ($> 4.0°$C) and/or high S_{BOT} (> 32.0) suggested that the water columns were composed by warmer ACW at the surface and/or high salinity BSW/AW at the bottom. PC3 was higher in 2007 than in 2008 and 2013, especially at the stations in the north of Bering Strait (Fig. 3), indicating that warm BSW and warmer ACW in upper layer and/or higher salinity AW or BSAW or DW in bottom layer.

3.2 Copepods abundance

The abundance of copepods at each station ranged between 150 and 146 323 inds. m^{-2} (median: 14 488). Large Arctic copepods (Cop$_{arc}$-L) included only *Calanus glacialis* (Table 2), occupied 0.00–48.2 % and found almost all over the study area. Cop$_{arc}$-L were more abundant in 2013 than in 2007 and 2008 (Fig. 4). Small Arctic copepods (Cop$_{arc}$-S) composed 1.47–55.6 % in number at each station and included *Pseudocalanus* spp, *P. minutus*, *P. mimus*, *P. newmani* and *P. acuspes* (Table 2). Cop$_{arc}$-S were dominant all over the study area in all study seasons (Fig. 4). Pacific copepods (Cop$_{pac}$) included *C. marshallae*, *N. cristatus*, *N. flemingeri*, *N. plumchrus*, *E. bungii* and *M. pacifica*. Cop$_{pac}$ were more abundant in the south ($< 69°$ N) than north in all study periods (Fig. 4).

3.3 Habitats of copepods

We constructed the habitat models using the anomaly of the timing of sea-ice retreat (aTSR), quantitative index of water masses (PC1, PC2 and PC3), bottom depth (Bdepth) and averaged log-transformed chlorophyll a in upper layer (Chl.a_{UPP}) and bottom layer (Chl.a_{BOT}) as potential explanatory variables. Averaged physical factors in upper layer and bottom layers were excluded from potential explanatory variables, as these were already included in the quantitative index of water masses.

The most adequate model explaining the abundance of Cop$_{arc}$-L included all explanatory variables (Table 5). Cop$_{arc}$-L were abundant at the station with the lower aTSR (< 0 days), with deeper Bdepth, especially in the area where the bottom depth was deeper than 45 m (Fig. 5). Cop$_{arc}$-L appeared to be abundant at stations with medium–higher PC1 (> -0.5), low–high PC2 (-1–1), low–medium PC3 (-1–0). The abundance of Cop$_{arc}$-L was slightly high in the water of low (< -0.5) and high (0.2–0.5) Chl.a_{UPP}, however, the effects of Chl.a_{UPP} and Chl.a_{BOT} on Cop$_{arc}$-L were not clear.

The most adequate model explaining the abundance of Cop$_{arc}$-S included all explanatory variables except PC2 (Table 5). Cop$_{arc}$-S were abundant at the station with the lower aTSR (< 5 days), with deeper Bdepth, especially in the area where the sea depth was deeper than 40 m (Fig. 5). The abundance of Cop$_{arc}$-S was high in low-high PC1 ranged from -1.5 to 2 and medium PC3 (0–1.2), and in medium–high Chl.a_{UPP} (> 0) (Fig. 5). The effect of Chl.a_{BOT} was not clear on the abundance of Cop$_{arc}$-S.

The most adequate model explaining the abundance of Cop$_{pac}$ included all explanatory variables except Chl.a_{UPP} (Table 5). Cop$_{pac}$ were abundant at stations with low aTSR (< 0 days), deeper Bdepth with clear positive effects in waters deeper than 35 m, low–medium PC1 (-2–0.5) and PC3 (-0.5–1) and PC2 (< -0.5), and less abundant at stations with medium–high PC2 (> -0.5) and high PC1 (> 0.5) (Fig. 5). The abundance of Cop$_{pac}$ was high in the water of low (< -0.2) and high (> 0.5) Chl.a_{BOT}, however, the effects of Chl.a_{BOT} on Cop$_{pac}$ was not clear.

4 Discussion

4.1 The application of principal component analysis

In the northern Bering Sea and Chukchi Sea, the major six water mass (Alaskan coastal water (ACW), ice melt water (IMW) and dense water (DW), Bering Shelf water (BSW), Anadyr water (AW) and merged Bering Shelf Anadyr water (BSAW)) are dominated (e.g., Coachman et al., 1975; Springer et al., 1989). These water masses and their combinations have mostly been described by clustered analysis using temperature and salinity (e.g., Norcross et al., 2010; Eisner et al., 2013; Ershova et al., 2015). This study quantitatively characterized these water masses using PCA; the combination of water masses, the number of composing layers (single or double layered) and the occurrence of high salinity water in bottom layer and/or warm water in upper layer (Fig. 2), quantitatively.

In the summer of 2008 and 2013, the northern part of the Chukchi Sea ($> 69°$ N) was dominated by the double-layered water mass with the cold ($< 0.0\,°$C)/lower salinity (< 30.0) IMW in the upper layer and colder ($< -1.0\,°$C)/high salinity (32.0–33.0) DW in the bottom layer, giving high PC1 (> 1.0), low–medium PC2 (< 0.5) and medium PC3 (-1.0–1.0) (Fig. 3). In these two years, the southern part of the Chukchi Sea ($< 69°$ N) and the Bering Strait were characterized by single layered structure with cold (-1.0–1.5 °C)/high salinity (32.5–33.0) AW and warm (0.0–10.0 °C)/high salinity (31.8–32.5) BSW, or BSAW, giving low–medium PC1 (-1.5–1.0), medium–high PC2 (> 0.5) and low PC3 (< -1.0) (Fig. 3). In the summer of 2007, however, the water off Point Hope (southern part of the Chukchi Sea) was characterized by warmer (2.0–10 °C)/low salinity (< 31.8) ACW as upper layer and AW as bottom layer (Figs. 2 and 3), giving low PC1 (< -1.5), medium–high PC2 (> 0.5) and low PC3 (< -1) (Fig. 3). Combination and distributions of water masses are known to be affected by Pacific inflow (Weingartner et al., 2005) and related to sea-ice retreats (Coachman et al., 1975; Day et al., 2010). This indicates that the inflow of warmer Pacific ACW was dominated in 2007 (Woodgate et al., 2010), and this strong inflow was believed to trigger of sea-ice retreat

Distribution of Arctic and Pacific copepods and their habitat

H. Sasaki et al.

Title Page

Abstract | Introduction

Conclusions | References

Tables | Figures

◀ | ▶

◀ | ▶

Back | Close

Full Screen / Esc

Printer-friendly Version

Interactive Discussion

in the western Arctic Ocean (Woodgate et al., 2012). Thus, variability of water masses and its combination indexed by PCs were agreed with the conventional description of the dynamics of water masses. Our index can be used to evaluate the effects of water mass combination with multiple components of water properties quantitatively and so be useful for predicting the distribution of copepods under climate changes.

4.2 Habitats of copepods

In the northern Bering Sea and Chukchi Sea, it has been well documented that the community structure and the abundance of zooplankton species were varied in water masses (e.g., Lane et al., 2008; Hopcroft et al., 2010; Matsuno et al., 2011). The abundance of all copepod groups in this study was also related to water mass (Fig. 5). For example, large Arctic copepods (Cop_{arc}-L) were slightly abundant in the water with cold/lower salinity IMW at upper layer and the colder/high salinity DW in bottom layer corresponding to higher PC1 and low–medium PC2 and PC3, or cold/high–higher salinity BSAW and AW in both layer corresponding to medium PC1, medium–high PC2 and low–medium PC3. These observations support the previous findings that *C. glacialis* in the Arctic population is distributed in Winter Water (Ershova et al., 2015) and concentrated further offshore in higher salinity BSAW at the bottom (Eisner et al., 2013). However, Cop_{arc}-L in this study were less abundant in ACW at upper layer and BSAW at the bottom layer corresponding to low–medium PC1 and high–medium PC3 (Fig. 5). This contradicted with Eisner et al. (2013) that found that *C. glacialis* was more abundant in the water with BSAW at the bottom and ACW at the upper layer.

In contrast to Cop_{arc}-L, small Arctic copepods (Cop_{arc}-S) were common through the study area, they were abundant in waters of medium PC1 medium PC3, indicating that this group is distributed in waters having wide range of temperature and saline, i.e., warm/saline BSW. However, Cop_{arc}-S were less abundant in the waters of higher PC1, i.e., colder/low salinity IMW at upper layer and cold/high salinity DW. These support the previous findings that small Arctic copepods (e.g., *Pseudocalunus* sp., *A. Hudson-*

18673

ica and *A.longiremis*) were abundant in warm BSW and warmer ACW at either upper and/or bottom layers (Eisner et al., 2013; Ershova et al., 2015).

Thus, abundance of Cop_{arc}-L could be associated with cold water mass where Cop_{arc}-S were less abundant. The difference in water masses between Cop_{arc}-L and Cop_{arc}-S might be related to body size and life cycle. Cop_{arc}-S are smaller and have multiple generations per year (e.g., McLaren et al., 1989), while Cop_{arc}-L have 1–3 year life cycle (Melle et al., 1998). Larger Cop_{arc}-L can accumulate more lipid than Cop_{arc}-S and larger energy storage enables Cop_{arc}-L to diapause under sea-ice in winter (Seuthe et al., 2007; Falk-Peterson et al., 2009) and to be active and graze ice-algae under the sea-ice in cold IMW and DW in pring. Although few studies about lipid of smaller-sized copepods (e.g., Kattner and Hagen, 2009), Cop_{arc}-S might not be able to diapause so long time in cold water because of their small body size, so abundant in the warmer ACW in upper and higher nutrient BSW in bottom layers.

Pacific zooplanktons are advected into the western Arctic Ocean through the Bering Strait (Springer et al., 1989). Previous studies showed that Pacific zooplankton communities were observed in the high salinity water (BSW/AW) in the northern Bering Sea and Chukchi Sea (Springer et al., 1989; Lane et al., 2008; Hopcroft et al., 2010; Matsuno et al., 2011; Eisner et al., 2013). In this study, Pacific copepods (Cop_{pac}) were abundant in the Bering Strait and Chukchi Sea south of Point Hope, giving low-medium PC1 and PC2; associated with warmer/low salinity ACW in upper layer and cold/higher salinity AW and warm/saline BSW or BSAW in the bottom layer, or single layered AW, BSW and BSAW, supporting these previous observations. Our study further confirmed the effects of the interannual variation of the water masses on the abundance of copepods. During the summer of 2007, Pacific water masses (ACW, BSW and BSAW) extended to the north of 69° N (Fig. 3) and transported Cop_{pac} into the Chukchi Sea (Matsuno et al., 2011). But in the summer of 2008 and 2013 when IMW and colder/high salinity DW were dominant, and little Cop_{pac} were collected in the northern part of the Chukchi Sea (Fig. 4).

4.3 Effects of sea-ice, phytoplankton and bottom depth

The influences of the changes in sea-ice on Arctic and subarctic ecosystem have been implicated in several previous studies about phytoplankton, benthic and higher trophic level organisms (Arrigo et al., 2008; Moore and Huntington, 2008; Grebmeier et al., 2012). In this study, the positive effects of earlier sea-ice retreat on the abundance of all copepod groups have shown in the result of GAM (Fig. 5). There has been little study that captures the influence of the timing of sea-ice retreat on the abundance of copepods, whereas the relationship between sea-ice retreat timing and the phytoplankton bloom has been well discussed in previous studies (e.g., Hunt et al., 2002, 2010; Kahru et al., 2010; Brown et al., 2011). The timing of phytoplankton bloom which is affected by the timing of sea-ice retreat plays an important role in the recruitment of copepods in the southeastern Bering Sea (Hunt et al., 2002, 2011; Overland and Stabeno, 2004; Stabeno et al., 2007). Brown and Arrigo (2013) showed the spring bloom inevitably formed at the ice edge and its timing was controlled by the timing of sea-ice retreat in the northern Bering Sea. In addition, Sigler et al. (2014) suggested that no ice-associated bloom occurs under the earlier sea-ice retreats (before mid-March), because sunlight is not sufficient to an ice-associated bloom throughout the eastern Bering Sea. In these years with earlier sea-ice retreat, the spring bloom occurs in late spring (May–early June) (Sigler et al., 2014). In the late spring bloom with warmer temperature, grazing by copepods can increase. Thus, earlier sea-ice retreat might have positive effects on reproduction of copepods in the northern Bering Sea and Chukchi Sea.

Cop$_{arc}$-S (e.g., *Pseudocalanus* spp.) graze phytoplankton and reproduce in the surface layer during day and night in summer (Norrbin et al., 1996; Plourde et al., 2002; Harvey et al., 2009). We, therefore, expected positive effects of the surface chlorophyll *a* concentration (Chl.a_{UPP}) on abundance of Cop$_{arc}$-S. The obvious relationships between the abundance of copepods, however, Chl.a_{UPP} were not observed. Plausible explanation is that the sampling period (June–August) might not coincide with the

high-grazing and reproduction season when they require large amount of food intake. Cop_{arc}-L reproduce during the spring phytoplankton bloom (e.g., Falk-Peterson et al., 2009), so our sampling period was not the time of their reproduction. The phytoplankton cells sinking into the bottom layers might be important food for copepods (Sameoto et al., 1986). Thus we also expected positive effects of the bottom chlorophyll a concentration ($Chl.a_{BOT}$) on all copepod groups. However, clear positive effects were not observed again (Fig. 5). It is difficult to link chlorophyll a concentration to copepod abundance using time lag between the bloom of phytoplankton and copepods.

There were a few previous studies reporting the associations between the abundance of copepods and the bottom depth in shelf of the northern Bering Sea and Chukchi Sea (e.g., Ashjian et al., 2003). The reason why all copepod groups were less abundant in waters shallower than 32 m bottom depth was unclear. These sampling stations were near the land with relative low salinity ($\rho = 0.53$, spearman's rank correlation test in S_{UPP} vs. Bdepth $p < 0.01$). Although oceanic copepods survive in waters 0–25 m bottom depth with low salinity in the Arctic Canada basin (Kosobokova and Hopcroft, 2010), the sallower area in this study was considered to be affected by fresh waters from land and unsuitable for all copepods.

The association between environmental factors and the abundance of copepods and its communities have been well documented (e.g., Springer et al., 1989; Lane et al., 2008; Matsuno et al., 2011). Recently these relationships have been analyzed using clustered water masses (Eisner et al., 2013; Ershova et al., 2015). This study indexed the water mass and then modelled the relationship between the water mass characteristics and spatial patterns of copepods abundance quantitatively. Our evaluation of the changes in the timing of sea-ice retreat on the abundance of copepods insisted the suitable environment for copepods are forming by the early sea-ice retreat. The influence of the changes in sea-ice in Arctic ecosystem has been well documented. However, to the best of our understanding, this is the first quantitative study to show the relationships between the early sea-ice retreat and the abundance of copepods. Quantitative analyses using the habitat models are useful for understanding various

phenomena and risks faced by organisms (e.g., sea-ice loss, increased water temperature and fresh water content). Furthermore, it can be adapted to predict the changes on ecosystem in future by incorporating climate and predicted environmental data. It can also be used to understand the responses of organisms to environmental change in the northern Bering Sea and Chukchi Sea.

References

Arrigo, K. R., van Dijken, G., and Pabi, S.: Impact of a shrinking Arctic ice cover on marine primary production, Geophys. Res. Lett., 35, L19603, doi:10.1029/2008GL035028, 2008.

Ashjian, C. J., Campbell, R. G., Welch, H. E., Butler, M., and Van Keuren, D.: Annual cycle in abundance, distribution, and size in relation to hydrography of important copepod species in the western Arctic Ocean, Deep-Sea Res. Pt. I, 50, 1235–1261, 2003.

Brown, Z. W. and Arrigo, K. R.: Sea ice impacts on spring bloom dynamics and net primary production in the Eastern Bering Sea, J. Geophys. Res.-Oceans, 118, 43–62, 2013.

Brown, Z. W., van Dijken, G. L., and Arrigo, K. R.: A reassessment of primary production and environmental change in the Bering Sea, J. Geophys. Res.-Oceans, 116, doi:10.1029/2010JC006766, 2011.

Clement, J. L., Cooper, L. W., and Grebmeier, J. M.: Late winter water column and sea ice conditions in the northern Bering Sea, J. Geophys. Res.-Oceans, 109, doi:10.1029/2003JC002047, 2004.

Coachman, L. K., Aagaard, K., and Tripp, R. B.: Bering Strait: the regional physical oceanography, University of Washington Press, Seattle, 1975.

Comiso, J. C., Parkinson, C. L., Gersten, R., and Stock, L.: Accelerated decline in the Arctic sea ice cover, Geophys. Res. Lett., 35, L01703, doi:10.1029/2007GL031972, 2008.

Day, R. H., Weingartner, T. J., Hopcroft, R. R., Aerts, L. A. M., Blanchard, A. L., Gall, A. E., Gallaway, B. J., Hannay, D. E., Holladay, B. A., Mathis, J. T., Norcross, B. L., Questel, J. M., and Wisdom, S. S.: The offshore northeastern Chukchi Sea, Alaska: a complex high-latitude ecosystem, Cont. Shelf Res., 67, 147–165, 2013.

Doney, S. C., Ruckelshaus, M., Duffy, J. E., Barry, J. P., Chan, F., English, C. A., Galindo, H. M., Grebmeier, J. M., Hollowed, A. B., Knowlton, N., Polovina, J., Rabalais, N. N., Sydeman, W. J., and Talley, L. D.: Climate change impacts on marine ecosystems, Ann. Rev. Mar. Sci., 4, 11–37, 2012.

Dvoretsky, V. and Dvoretsky, A.: Life cycle of *Oithona similis* (Copepoda: Cyclopoida) in Kola Bay (Barents Sea), Mar. Biol., 156, 1433–1446, 2009.

Eisner, L., Hillgruber, N., Martinson, E., and Maselko, J.: Pelagic fish and zooplankton species assemblages in relation to water mass characteristics in the northern Bering and southeast Chukchi seas, Polar Biol., 36, 87–113, 2013.

Ershova, E. A., Hopcroft, R. R., and Kosobokova, K. N.: Inter-annual variability of summer mesozooplankton communities of the western Chukchi Sea: 2004–2012, Polar Biol., 38, 1461–1481, 2015.

Falk-Petersen, S., Mayzaud, P., Kattner, G., and Sargent, J. R.: Lipids and life strategy of Arctic *Calanus*, Mar. Biol. Res., 5, 18–39, 2009.

Grebmeier, J. M.: Shifting patterns of life in the Pacific Arctic and sub-Arctic seas, Ann. Rev. Mar. Sci., 4, 63–78, 2012.

Grebmeier, J. M., Overland, J. E., Moore, S. E., Farley, E. V., Carmack, E. C., Cooper, L. W., Frey, K. E., Helle, J. H., McLaughlin, F. A., and McNutt, S. L.: A major ecosystem shift in the northern Bering Sea, Science, 311, 1461–1464, 2006.

Grebmeier, J. M., Moore, S. E., Overland, J. E., Frey, K. E., and Gradinger, R.: Biological response to recent Pacific Arctic sea ice retreats, Eos, Trans. Am. Geophys. Union, 91, 161–162, 2010.

Distribution of Arctic and Pacific copepods and their habitat

H. Sasaki et al.

Title Page

Abstract	Introduction
Conclusions	References
Tables	Figures

|◄   ►|

◄   ►

Back   Close

Full Screen / Esc

Printer-friendly Version

Interactive Discussion

Harvey, M., Galbraith, P. S., and Descroix, A.: Vertical distribution and diel migration of macro-zooplankton in the St. Lawrence marine system (Canada) in relation with the cold intermediate layer thermal properties, Prog. Oceanogr., 80, 1–21, 2009.

Hopcroft, R. R. and Kosobokova, K. N.: Distribution and egg production of *Pseudocalanus* species in the Chukchi Sea, Deep-Sea Res. Pt. II, 57, 49–56, 2010.

Hopcroft, R. R., Kosobokova, K. N., and Pinchuk, A. I.: Zooplankton community patterns in the Chukchi Sea during summer 2004, Deep-Sea Res. Pt. II, 57, 27–39, 2010.

Hunt, G. L., Stabeno, P., Walters, G., Sinclair, E., Brodeur, R. D., Napp, J. M., and Bond, N. A.: Climate change and control of the southeastern Bering Sea pelagic ecosystem, Deep-Sea Res. Pt. I, 49, 5821–5853, 2002.

Hunt, G. L., Coyle, K. O., Eisner, L. B., Farley, E. V., Heintz, R. A., Mueter, F., Napp, J. M., Overland, J. E., Ressler, P. H., and Salo, S.: Climate impacts on eastern Bering Sea foodwebs: a synthesis of new data and an assessment of the Oscillating. Control. Hypothesis., ICES, J. Mar. Sci. Technol., 68, 1230–1243, 2011.

Hunt, G. L., Blanchard, A. L., Boveng, P., Dalpadado, P., Drinkwater, K. F., Eisner, L., Hopcroft, R. R., Kovacs, K. M., Norcross, B. L., and Renaud, P.: The Barents and Chukchi Seas: comparison of two Arctic shelf ecosystems, J. Marine Syst., 109, 43–68, 2013.

Iken, K., Bluhm, B., and Dunton, K.: Benthic food-web structure under differing water mass properties in the southern Chukchi Sea, Deep-Sea Res. Pt. II, 57, 71–85, 2010.

Kahru, M., Brotas, V., Manzano-Sarabia, M., and Mitchell, B. G.: Are phytoplankton blooms occurring earlier in the Arctic?, Glob. Change Biol, 17, 1733–1739, 2011.

Kattner, G. and Hagen, W.: Lipids in marine copepods: latitudinal characteristics and perspective to global warming, in: Lipids in Aquatic Ecosystems, Springer, 257–280, 2009.

Kosobokova, K. N. and Hopcroft, R. R.: Diversity and vertical distribution of mesozooplankton in the Arctic's Canada Basin, Deep-Sea Res. Pt. II, 57, 96–110, 2010.

Lane, P. V. Z., Llinás, L., Smith, S. L., and Pilz, D.: Zooplankton distribution in the western Arctic during summer 2002: Hydrographic habitats and implications for food chain dynamics, J. Marine Syst., 70, 97–133, 2008.

Lowry, L. F., Sheffield, G., and George, J. C.: Bowhead whale feeding in the Alaskan Beaufort Sea, based on stomach contents analyses, J. Cetacean Res. Manage., 6, 215–223, 2004.

Matsuno, K., Yamaguchi, A., Hirawake, T., and Imai, I.: Year-to-year changes of the mesozooplankton community in the Chukchi Sea during summers of 1991, 1992 and 2007, 2008, Polar Biol., 34, 1349–1360, 2011.

Title Page

Abstract | Introduction

Conclusions | References

Tables | Figures

Back | Close

Full Screen / Esc

Printer-friendly Version

Interactive Discussion

Matsuno, K., Yamaguchi, A., Hirawake, T., Nishino, S., Inoue, J., and Kikuchi, T.: Reproductive success of Pacific copepods in the Arctic Ocean and the possibility of changes in the Arctic ecosystem, Polar Biol., 38, 1075–1079, 2015.

McLaren, I., Laberge, E., Corkett, C., and Sevigny, J.-M.: Life cycles of four species of *Pseudocalanus* in Nova Scotia, Can. J. Zoo., 67, 552–558, 1989.

Melle, W. and Skjoldal, H.: Reproduction and development of *Calanus finmarchicus*, *C. glacialis* and *C. hyperboreus* in the Barents Sea, Mar. Ecol.-Prog. Ser., 169, 211–228, 1998.

Moore, S. E. and Huntington, H. P.: Arctic marine mammals and climate change: impacts and resilience, Ecol. Appli., 18, 157–165, 2008.

Mueter, F. J. and Litzow, M. A.: Sea ice retreat alters the biogeography of the Bering Sea continental shelf, Ecol. Appli., 18, 309–320, 2008.

Nakano, T., Matsuno, K., Nishizawa, B., Iwahara, Y., Mitani, Y., Yamamoto, J., Sakurai, Y., and Watanuki, Y.: Diets and body condition of polar cod (*Boreogadus saida*) in the northern Bering Sea and Chukchi Sea, Polar Biol., 1–6, doi:10.1007/s00300-015-1769-x, 2015.

Norcross, B. L., Holladay, B. A., Busby, M. S., and Mier, K. L.: Demersal and larval fish assemblages in the Chukchi Sea, Deep-Sea Res. Pt. II, 57, 57–70, 2010.

Norrbin, M., Davis, C., and Gallager, S.: Differences in fine-scale structure and composition of zooplankton between mixed and stratified regions of Georges Bank, Deep-Sea Res. Pt. II, 43, 1905–1924, 1996.

Overland, J. E. and Stabeno, P. J.: Is the climate of the Bering Sea warming and affecting the ecosystem?, Eos, Transactions American Geophysical Union, 85, 309–312, 2004.

Parkinson, C. L. and Comiso, J. C.: On the 2012 record low Arctic sea ice cover: combined impact of preconditioning and an August storm, Geophys. Res. Lett., 40.7, 1356–1361, doi:10.1002/grl.50349, 2013.

Piatt, J. F. and Springer, A. M.: Advection, pelagic food webs and the biogeography of seabirds in Beringia, Mar. Ornith., 31, 141–154, 2003.

Plourde, S., Dodson, J. J., Runge, J. A., and Therriault, J.-C.: Spatial and temporal variations in copepod community structure in the lower St. Lawrence Estuary, Canada, Mar. Ecol.-Prog. Ser., 230, 211–224, 2002.

Sameoto, D., Herman, A., and Longhurst, A.: Relations between the thermocline meso and microzooplankton, chlorophyll a and primary production distributions in Lancaster Sound, Polar Biol., 6, 53–61, 1986.

Seuthe, L., Darnis, G., Riser, C. W., Wassmann, P., and Fortier, L.: Winter–spring feeding and metabolism of Arctic copepods: insights from faecal pellet production and respiration measurements in the southeastern Beaufort Sea, Polar Biol., 30, 427–436, 2007.

Shimada, K., Kamoshida, T., Itoh, M., Nishino, S., Carmack, E., McLaughlin, F., Zimmermann, S., and Proshutinsky, A.: Pacific Ocean inflow: influence on catastrophic reduction of sea ice cover in the Arctic Ocean, Geophys. Res. Lett., 33, L08605, doi:10.1029/2005GL025624, 2006.

Sigler, M. F., Stabeno, P. J., Eisner, L. B., Napp, J. M., and Mueter, F. J.: Spring and fall phytoplankton blooms in a productive subarctic ecosystem, the eastern Bering Sea, during 1995–2011, Deep-Sea Res. Pt. II, 109, 71–83, 2014.

Springer, A. M., McRoy, C. P., and Turco, K. R.: The paradox of pelagic food webs in the northern Bering Sea – II. Zooplankton communities, Cont. Shelf Res., 9, 359–386, 1989.

Springer, A. M., McRoy, C. P., and Flint, M. V.: The Bering Sea Green Belt: shelf-edge processes and ecosystem production, Fish. Oceanogra., 5, 205–223, 1996.

Stabeno, P., Bond, N., and Salo, S.: On the recent warming of the southeastern Bering Sea shelf, Deep-Sea Res. Pt. II, 54, 2599–2618, 2007.

Suzuki, R. and Ishimaru, T.: An improved method for the determination of phytoplankton chlorophyll using N, N-dimethylformamide, J. Oceanogr. Soc. Japan, 46, 190–194, 1990.

Weingartner, T., Aagaard, K., Woodgate, R., Danielson, S., Sasaki, Y., and Cavalieri, D.: Circulation on the north central Chukchi Sea shelf, Deep-Sea Res. Pt. II, 52, 3150–3174, 2005.

Weingartner, T., Dobbins, E., Danielson, S., Winsor, P., Potter, R., and Statscewich, H.: Hydrographic variability over the northeastern Chukchi Sea shelf in summer-fall 2008–2010, Cont. Shelf Res., 67, 5–22, 2013.

Welschmeyer, N. A.: Fluorometric analysis of chlorophyll *a* in the presence of chlorophyll *b* and pheopigments, Limnol. Oceanogr., 39, 1985–1992, 1994.

Woodgate, R. A., Weingartner, T., and Lindsay, R.: The 2007 Bering Strait oceanic heat flux and anomalous Arctic sea - ice retreat, Geophys. Res. Lett., 37, L01602, doi:10.1029/2009GL041621, 2010.

Woodgate, R. A., Weingartner, T. J., and Lindsay, R.: Observed increases in Bering Strait oceanic fluxes from the Pacific to the Arctic from 2001 to 2011 and their impacts on the Arctic Ocean water column, Geophys. Res. Lett., 39, L24603, doi:10.1029/2012GL054092, 2012.

Table 1. Water mass properties in the northern Bering Sea and Chukchi Sea.

Water mass	Temperature	Salinity	Reference
Alaskan coastal water (ACW)	warmer (2.0–13.0 °C)	low salinity (< 31.8)	Coachman et al. (1975) Walsh (1989)
Bering Shelf Water (BSW)	warm (0.0–10.0 °C)	saline (31.8–32.5)	Coachman et al. (1987) Springer et al. (1989) Grebmeier et al. (1988)
Anadyr water (AW)	cold (−1.0–1.5 °C)	higher salinity (32.5–33.3)	Coachman et al. (1987) Springer et al. (1989) Grebmeier et al. (1988)
Bering Shelf Anadyr water (BSAW)	cold (−1.0–2.0 °C)	high salinity (31.8–33.0)	Grebmeier et al. (1989) Feder et al. (2007) Eisner et al. (2013)
ice melt water (IMW)	cold (< 2.0 °C)	lower salinity (< 30.0)	Feder et al. (1989)
dense water (DW)	colder near-freezing (< −1.0 °C)	high salinity (32.0–33.0)	Coachman et al. (1975) Feder et al. (1994) Weingartner et al. (2010)

Table 2. The copepods species included in each copepod groups: large Arctic (Cop$_{arc}$-L), small Arctic (Cop$_{arc}$-S) and Pacific (Cop$_{pac}$) copepods.

Response Variables	Description	Species
Cop$_{arc}$-L Cop$_{arc}$-S	large size Arctic copepods small size Arctic copepods	*Calanus glacialis* *Acartia hudsonica* *Acartia longiremis* *Acartia tumida* *Centropages abdominalis* *Eurytemora herdmani* *Epilabidocera amphitrites* *Microcalanus pygmaeus* *Pseudocalanus acuspes* *Pseudocalanus mimus* *Pseudocalanus minutus* *Pseudocalanus newmani* *Pseudocalanus* spp. *Scolecithricella minor* *Tortanus discaudatus* Cyclopoid copepods
Cop$_{pac}$	Pacific copepods	*Calanus marshallae* *Eucalanus bungii* *Metridia pacifica* *Neocalanus cristatus* *Neocalanus flemingeri* *Neocalanus plumchrus*

Table 3. The covariates for principal component analysis and explanatory variables for Generalize Additive Models (GAMs).

Explanatory variable in GAM	Environmental Variables	Description	Unit
The principal components (PC1, PC2 and PC3)	$\frac{d\rho}{dD}_{max}$	Magnitude of the maximam potential density gradient	g m^{-1}
	T_{UPP}	Vertical averaged temperature above the depth of the maximam potential density gradient	˚C
	T_{BOT}	Vertical averaged temperature under the depth of the maximam potential density gradient	˚C
	S_{UPP}	Vertical averaged salinity above the depth of the maximam potential density gradient	
	S_{BOT}	Vertical averaged salinity under the depth of the maximam potential density gradient	
BDepth	Depth	Bottom depth	m
Chl a_{UPP}	Chl a_{UPP}	Vertical averaged log-transformed Chlorophyll a concentration above the depth of the maximam potential density gradient	
Chl a_{BOT}	Chl a_{BOT}	Vertical averaged log-transformed Chlorophyll a concentration under the depth of the maximam potential density gradient	
aTSR	aTSR	Temporal difference from the Timing of Sea ice Retreat (TSR) anomaly to TSR between 1991 and 2013	days

Distribution of Arctic and Pacific copepods and their habitat

H. Sasaki et al.

Title Page

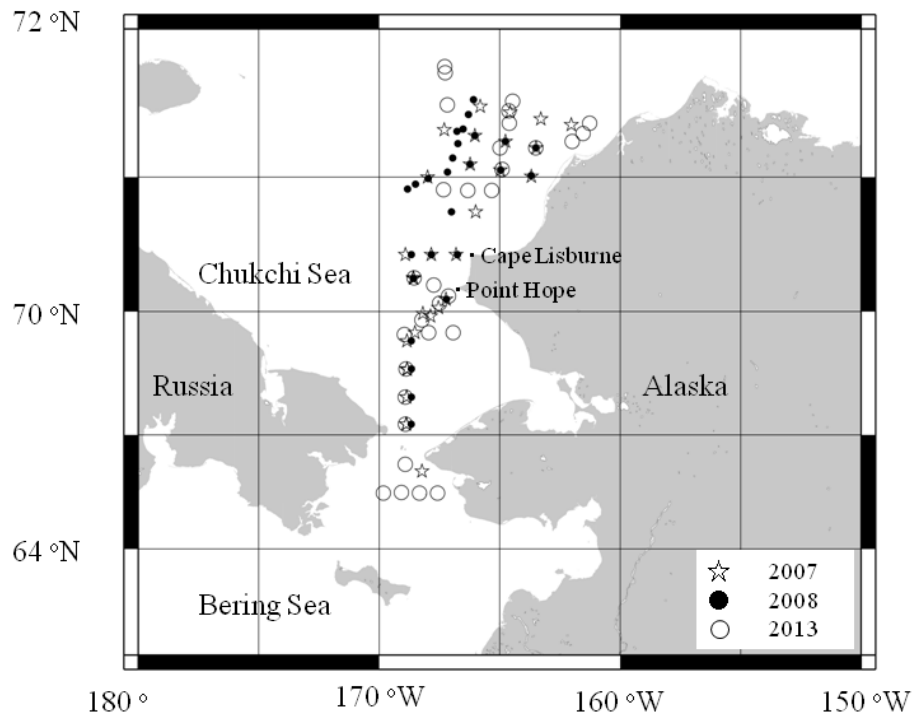Abstract | Introduction

Conclusions | References

Tables | Figures

|◄ | ►|

◄ | ►

Back | Close

Full Screen / Esc

Printer-friendly Version

Interactive Discussion

Table 4. Eigenvalue and factor loadings of principle component analysis. The variances and eigenvalue of each principal component (PC) are also given. Descriptions of elements are same as Table 2 (See Table 2).

Elements	Eigenvector (Factor loadings)									
	PC1		PC2		PC3		PCA4		PCA5	
$\frac{d\rho}{dD}\,\text{max}$	0.36	(0.55)	−0.55	(−0.73)	0.45	(0.38)	−0.27	(−0.10)	0.54	(0.15)
T_{UPP}	−0.51	(−0.78)	−0.38	(−0.50)	0.38	(0.32)	−0.38	(−0.13)	−0.56	(−0.15)
S_{UPP}	−0.43	(−0.66)	0.54	(0.71)	0.11	(0.09)	−0.54	(−0.19)	0.47	(0.13)
T_{BOT}	−0.60	(−0.92)	−0.18	(−0.24)	0.21	(0.18)	0.65	(0.23)	0.37	(0.10)
S_{BOT}	0.27	(0.41)	0.48	(0.63)	0.77	(0.65)	0.24	(0.08)	−0.21	(−0.06)
Eigenvalue	2.66		1.74		0.71		0.12		0.07	
Standard deviation	1.54		1.32		0.84		0.35		0.27	
Proportion of variance (%)	47.13		34.79		14.17		2.43		1.49	
Cumulative proportion (%)	47.13		81.92		96.08		98.51		100.00	

Table 5. Best models of each copepod groups: large Arctic (Cop_{arc}-L), small Arctic (Cop_{arc}-S) and Pacific (Cop_{pac}) copepods.

Response valiables	Best models	Deviance Explained (%)	Observed vs. Fitted R^2
Cop_{arc}-L	$s(aTSR)+ s(PC1)+ s(PC2)+ s(PC3)+ s(Chl\ a_{UPP})+ s(Chl\ a_{BOT})+ s(Bdepth\ ) + \epsilon$	92.4	0.94
Cop_{arc}-S	$s(aTSR)+ s(PC1)+ s(PC3)+ s(Chl\ a_{UPP})+ s(Chl\ a_{BOT})+ s(Bdepth\ ) + \epsilon$	89.9	0.88
Cop_{pac}	$s(aTSR)+ s(PC1)+ s(PC2)+ s(PC3)+ s(Chl\ a_{BOT})+ s(Bdepth\ ) + \epsilon$	75.3	0.38

Figure 1. Study area and sampling stations in the northern Bering Sea and Chukchi Sea during the summers of 2007, 2008 and 2013. The symbols denote the sampling stations where NORPAC net and CTD water samplings were conducted.
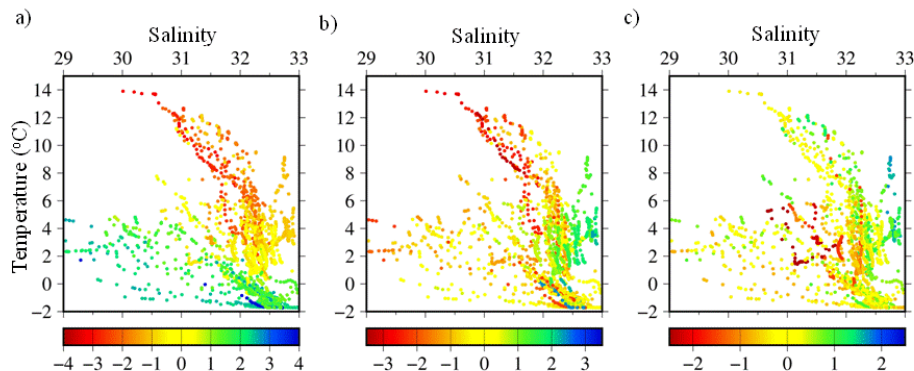
Figure 2. T–S diagrams of principal component scores **(a)** PC1, **(b)** PC2 and PC3 **(c)**. Colored circle indicated the magnitude of each PC. Water mass designations are Alaskan coastal water (ACW; salinity < 31.8 and temperature 2.0–13.0 °C), Bering Shelf Water (BSW; 31.8–32.5 and 0.0–10.0 °C), Anadyr Water (AW; 32.3–33.3 and -1.0–1.5 °C), Bering Shelf Anadyr water (BSAW; BSW and AW combined), ice melt water (IMW; < 30.0 and < 2.0 °C) and dense water (DW; 31.0–33.0 and < -1 °C).
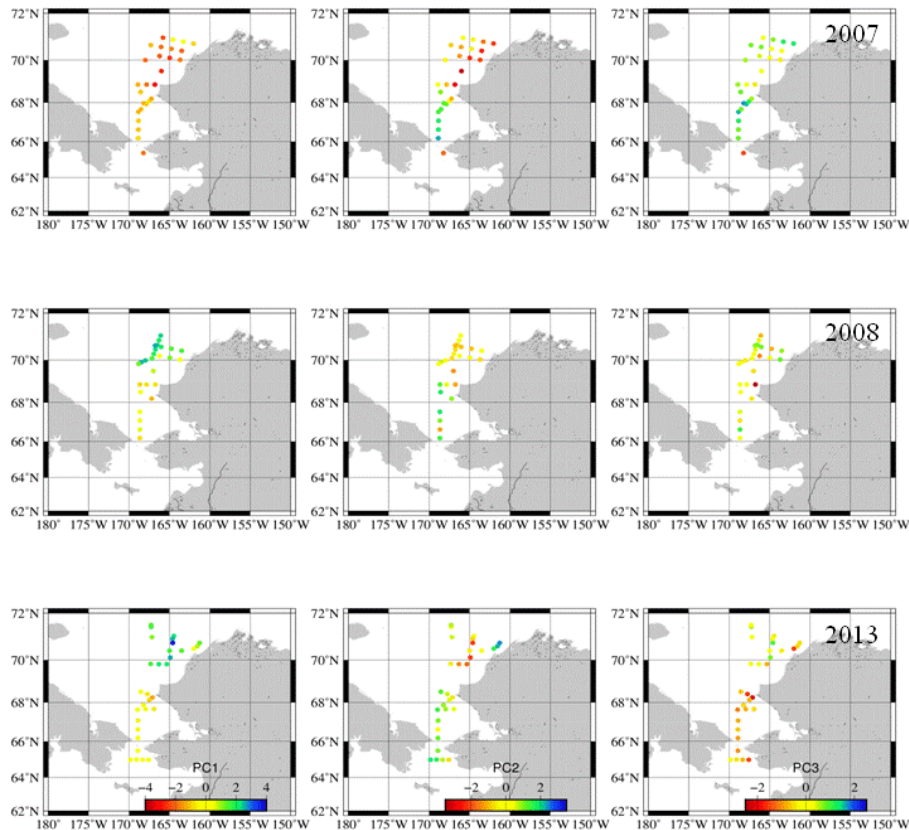
Figure 3. The distribution of main principal component score (PC1–3) in 2007, 2008 and 2013. Colored circles indicted the magnitude of PC.
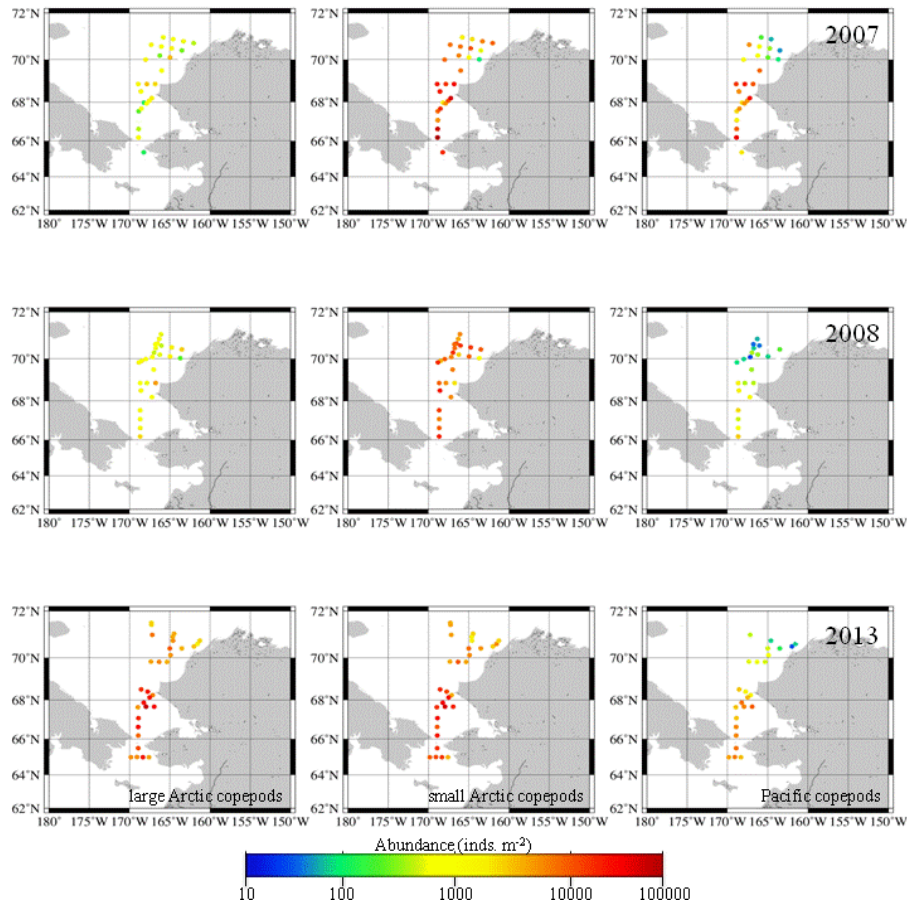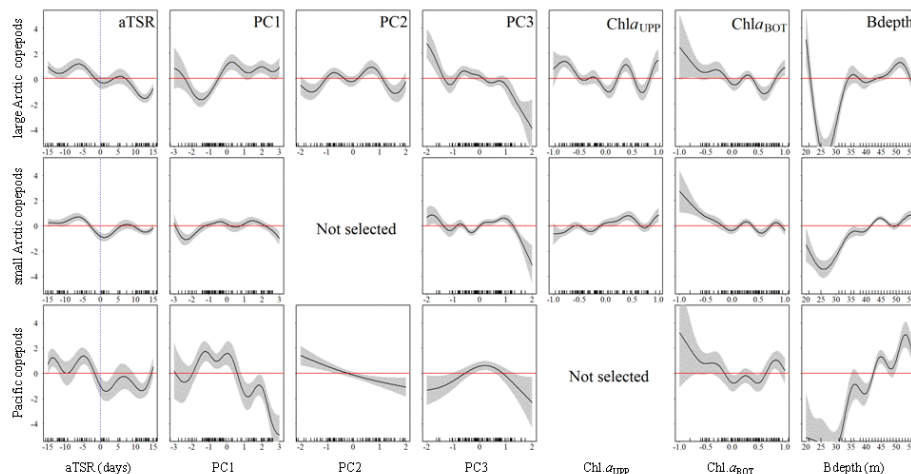
Figure 4. The distribution of copepods abundance in 2007, 2008 and 2013. Colored circles indicted the abundance of copepods: large Arctic (Cop$_{arc}$-L), small Arctic (Cop$_{arc}$-S) and Pacific (Cop$_{pac}$) copepods.

Title Page

Abstract | Introduction

Conclusions | References

Tables | Figures

◄ | ►►

◄ | ►

Back | Close

Full Screen / Esc

Printer-friendly Version

Interactive Discussion

Figure 5. GAM plot of the best model in each copepod groups: large Arctic (Cop$_{arc}$-L), small Arctic (Cop$_{arc}$-S) and Pacific (Cop$_{pac}$) copepods. The vertical axes indicate the estimate smoother for the abundance of copepods. The horizontal axes show the explanatory variable: the anomaly of the timing of sea-ice retreat (aTSR), principal component score (PC1–3) averaged log-transformed chlorophyll a concentration within the layer above and below $\frac{d\rho}{dD}$max (Chl a_{UPP} and Chl a_{BOT}) and bottom depth (Bdepth). Shade area represents 95 % confidence intervals. Short vertical lines located on the x axes of each plot indicate the values at which observations were made.